SIZE EFFECTS IN PROGRESSIVE DAMAGE OF NOTCHED AND HOLED COMPOSITES

B. Chen[1], T.E. Tay[1]*, P.M. Baiz[2] , S.T. Pinho[2]
1 Department of Mechanical Engineering, National University of Singapore, Singapore,
2 Department of Aeronautical Engineering, Imperial College London, London, UK
* Corresponding author (mpetayte@nus.edu.sg)

Keywords: *Size effect; cohesive model; thickness dependence of fracture energy*

1 Introduction

The strength dependence of notched composites on size of specimens has been well documented in literature. Wisnom et al. have performed extensive experimental studies on the size effect of V-notched and open-hole composite specimens under tension and compression [1-4]. It was shown that the strength of open-hole composite laminates depends on in-plane scale, thickness scale and ply lay-ups. Fiber direction mode I fracture energy has recently been experimentally determined to be thickness dependent in [5]. However, the mechanisms of this apparent dependence have not been fully explained. This paper presents a computational study of the prediction of in-plane strength of notched and holed laminates, accounting for the thickness size dependence effect, using a cohesive failure model..

2 Composite failure theory

2.1 Thickness dependence of composite fracture toughness

Literature reports large variations of the mode I fiber tensile fracture energy G_{fc} with respect to the thickness of the 0-plies in the tested specimen [5]. The amount of fiber pull-out in [02/90]s laminate increases compared to that in [0/90]s and causes a significant increase of energy dissipation. The measured 0-ply fracture energy of [02/90]s is more than twice of that of [0/90]s (Table 1). To the author's knowledge, no numerical work has employed this thickness dependence of fiber fracture energy. Although a quantitative description of mode I fiber fracture energy in terms of thickness has not been well established, for the cases in this project, only the fracture energies of single ply and two blocked plies are needed and they are available from [5]. The thickness dependence of fracture energy is applied to numerical modeling here and it will be shown later that this is critical to the prediction of thickness size effect.

2.2 Fiber failure modeling

Fiber tensile failure initiates when $\sigma_1 > X_t$ where X_t is the fiber direction lamina tensile strength. Post-failure softening of fiber tensile failure is modeled by a linear cohesive softening law (Fig.1). Fiber compressive failure is more complicated than tensile failure because fiber micro-buckling and kinking often happens before the material reaches its theoretical compressive strength, and the strength in compression is found to be very difficult to obtain in experiments [6, 7]. Current studies focus on tension problems and a simple maximum stress criterion $\sigma_1 < -X_c$ is used for fiber compressive failure initiation.

2.3 Matrix failure modeling

Matrix failure initiation is determined by Tsai-Wu failure criterion. Since this work studies tension loading cases and matrix here does not undergo compressive failure, only tension and shear stresses are involved in the failure criterion. It is also assumed that matrix cracks are all parallel to the fiber direction and perpendicular to the lamina shell plane (this assumption may not be valid for compressive failure since the shear fracture plane in compression generally will not be perpendicular to the lamina shell plane). Therefore the normal vector of potential crack surface is $\hat{e}_2$ and the stresses that apply to the potential crack surface are $\langle\sigma_2\rangle$, τ_{12} and τ_{32} where $\langle\sigma_2\rangle = \max(0, \sigma_2)$. σ_1 is kept as where it is in the original Tsai-Wu criterion form. The complete form of the matrix failure initiation criterion is:

$$F_1\sigma_1 + F_2\langle\sigma_2\rangle + F_{11}\sigma_1^{\,2} + F_{22}\langle\sigma_2\rangle^2 + F_{44}\tau_{32}^2 + F_{66}\tau_{12}^2 + 2F_{12}\sigma_1\langle\sigma_2\rangle = 1 \quad (1)$$

where $F_1 = \frac{1}{X_t} + \frac{1}{X_c}$, $F_{11} = -\frac{1}{X_t X_c}$, $F_2 = \frac{1}{Y_t} + \frac{1}{Y_c}$, $F_{22} = -\frac{1}{Y_t Y_c}$, $F_{44} = F_{66} = \frac{1}{S^2}$, $2F_{12} = -\sqrt{F_{11}F_{22}}$.[8]

Y_t is the matrix tensile strength and Y_c is the matrix compressive strength. S is the matrix shear strength. This form has an extra term $F_{44}\tau_{32}^2$ compared to classical plane-stress Tsai-Wu criterion. Numerical models here use continuum shell element which is formulated based on thick shell theory where transverse shear is considered. Since τ_{32} acts on the potential crack plane, it is therefore included in the criterion. The original derivation of Tsai-Wu criterion in [8] was based on 3D stress state and $F_{44} = \frac{1}{QQ'}$ where Q and Q' are positive and negative shear strengths along the 2-3 plane. Here the same shear strength is assumed for both positive and negative shear loadings and for both τ_{12} and τ_{32}, thus $F_{44} = F_{66} = \frac{1}{S^2}$.

Matrix damage propagation is described by a cohesive softening law of effective stress

$$\sigma_{eff} = \sqrt{\langle\sigma_2\rangle^2 + \tau_{12}^{\,2} + \tau_{23}^{\,2}} \quad (2)$$

with respect to effective displacement.

$$u_{eff} = l_e\sqrt{\langle\varepsilon_2\rangle^2 + \gamma_{12}^{\,2} + \gamma_{23}^{\,2}} \quad (3)$$

l_e is the characteristic element length. Mixed-mode fracture energy G_{mc} is defined by Benzeggagh-Kenane (B-K) formula [9]:

$$G_{mc} = G_n^C + (G_s^C - G_n^C)B^\eta \quad (4)$$

where

$$B = \left\{\frac{G_S}{G_N + G_S}\right\} \quad (5)$$

$$G_N = \frac{1}{2}\langle\sigma_2\rangle\langle\varepsilon_2\rangle l_e, \qquad G_S = \frac{1}{2}(\tau_{12}\gamma_{12} + \tau_{23}\gamma_{23})l_e \quad (6)$$

G_n^C is the mode I matrix fracture energy and G_s^C is the mode II/III matrix fracture energy. η is set to 1.

2.4 Delamination modelling

The role of delamination on laminate strength has been extensively studied in experiments by Wisnom et al.[11]. It is observed that for in-plane loading, significant delamination can occur, which releases the stress concentration of the 0-plies and affects the overall strength of the laminate. It is therefore important to include delamination analysis even for in-plane loading simulation. Here delamination is modeled by inserting ABAQUS cohesive elements of very small thickness (0.001mm) between plies. The initiation of delamination is determined by a quadratic stress criterion. Propagation of delamination is modeled by a linear cohesive softening law with mixed-mode fracture energy defined by the B-K formula. Table 2 lists values of the material parameters used for cohesive elements.

Values of the penalty stiffness K_{nn} (normal), K_{ss} and K_{tt} (two shear directions) are assumed to be very high as to simulate perfect bonding before delamination (Fig.2). Special care should be taken when assigning values to the above parameters so as to ensure that damage growth is always positive, i.e., no healing of material is predicted[12]. A formula proposed in [12] states the relationship between K_{nn}, K_{ss} and K_{tt}:

$$K_{ss} = K_{tt} = K_{nn}\frac{G_n^C}{G_s^C}\left(\frac{S}{N}\right)^2 \quad (7)$$

In this project, K_{nn} = 5×10^7 N/mm^3 and K_{ss} = K_{tt} = 2.25×10^7 N/mm^3. Delamination modeling using cohesive elements is very sensitive to element size [13,14]. The element size must be small enough to

capture the stress gradient in the cohesive zone, i.e. element size must be smaller than cohesive zone length. Quantitative study of the mesh size effect in cohesive model and the determination of cohesive zone length can be found in [13]. The cohesive zone length l_{cz} can be estimated by:

$$l_{cz} = \min\left(\frac{E_2 G_n^C}{N^2}, \frac{G_{13} G_s^C}{S^2}, \frac{G_{23} G_s^C}{S^2}\right) \quad (8)$$

In this work, l_{cz} = 0.5 mm, calculated using values in Table 1 and Table 2. Therefore the size of cohesive elements at areas of interest (around the hole) must be smaller than 0.5 mm.

3 Simulation results

Continuum shell elements are used to model plies and cohesive elements are used to model interfaces. The failure model in 2.2 and 2.3 is written in ABAQUS UMAT subroutine. Since the two center 0-plies are blocked together, from Table 2 we can see that they have a fiber fracture energy value of 130 KJ/m^2 while that of the other plies is 50 KJ/m^2. Mesh objectivity of the model is first verified on a selected OHT case (thickness = 1mm, hole diameter = 3.175mm) with four different meshes for plies and three for interfaces (maximum cohesive element size is controlled to be smaller than 0.5 mm). Good agreement with experiment is achieved (Fig.3) and the failure pattern predictions are consistent for different meshes (Fig.4).

The model is then applied to a series of in-plane-scaled 4mm thick specimens to predict in-plane size effect. Good agreement with experimental data is achieved (Table 3) which shows that cohesive model is capable of predicting in-plane size effect of composite. Camanho et al. [15] have performed similar in-plane size effect study by using a Continuum Damage Mechanics (CDM) model with energy regularization. CDM with energy regularization model uses a different failure initiation criterion and a different softening curve from the present model. However both models ensure that the area under the stress/displacement curve equals fracture energy. It is also shown in Bažant's size effect study [16] that proper consideration of the energy dissipation during damage and fracture in the constitutive model is essential for predicting size effect of materials. Stress/strain based constitutive law does not have the energy balance consideration and is shown to be mesh-dependent in strength predictions [15].

Thickness size effect is then studied next. It can be seen in Table 4 that for same in-plane scaled specimens (hole diameter = 3.175mm), experiments report that strength decreases while sublaminates are blocked. The strength predictions by the proposed model are very close to the experimental values. Let's define the average fracture toughness of all 0 plies as

$$\overline{G}_{fc} = \frac{G_{fc}^b \times N^b + G_{fc}^s \times N^s}{N^b + N^s} \quad (9)$$

where N^s is the number of single 0 plies and N^b is the number of blocked 0 plies. G_{fc}^b = 130 KJ/m^2 and G_{fc}^s = 50 KJ/m^2 from Table 1. It can be seen that as the sublaminates are blocked, N^s increases while N^b remains equal to 2 (two plies at the center). Therefore blocking sublaminates would decrease $\overline{G}_{fc}$ and therefore decrease the strength of the laminate. The decrease of $\overline{G}_{fc}$ would slow down as more sublaminates are blocked and eventually reaching a constant value equal to G_{fc}^s . This corresponds well to the experimental observation that strength decreases by more than 12% from t=1mm to t=2mm while only 4.4% from t=2mm to t=4mm.

4 Conclusion

Size effect of notched composite is studied using a failure model with cohesive post-failure softening law. The apparent thickness dependence of composite fracture energy previously reported in experiments is applied to a numerical study of composite laminates with holes. It is shown that the cohesive model is capable of predicting the in-plane strength dependence on size of notched composite, and that the thickness dependence of mode I fiber fracture energy of composite should be taken into account in the models. A quantitative description of mode I fiber fracture energy in terms of thickness should be established in the future.

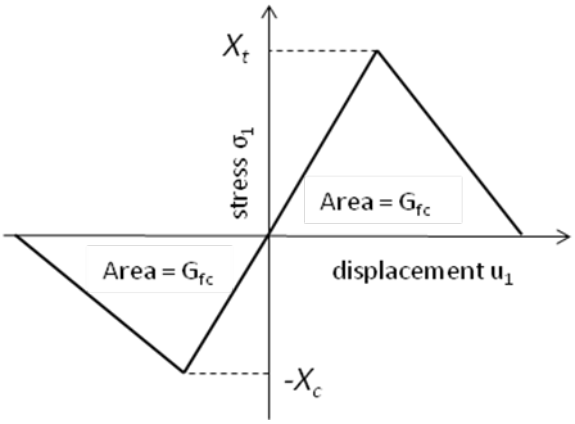

Fig.1. Cohesive linear softening law

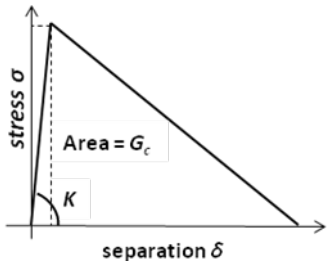

Fig.2. traction-separation law

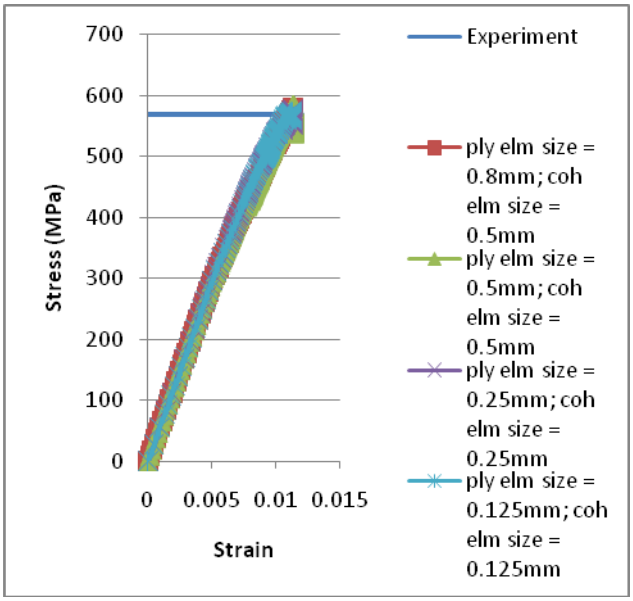

Fig.3. Mesh objectivity: stress-strain curves

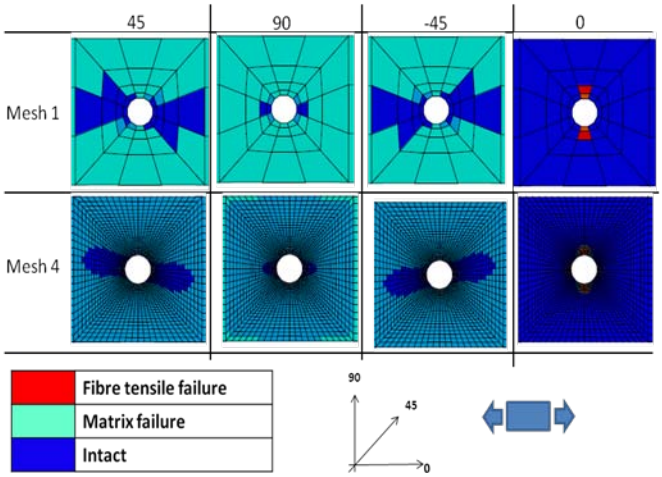

Fig.4. Mesh objectivity: damage patterns

Table 1. Lamina material (IM7/8552) parameters (from [3] unless specified)

E_1	$E_2 = E_3$	$\nu_{12}=\nu_{13}$	ν_{23}	$G_{12}=G_{13}$
161000 MPa	**11400 MPa**	**0.32**	**0.436**	**5170 MPa**
G_{23}	X_t (from [10])	X_c (from in-house experiment)	Y_t	Y_c (from in-house experiment)
3980 MPa	**2800 MPa**	**1725 MPa**	**60 MPa**	**228 MPa**
S	G_{fc} *(single ply)* (from [5])	G_{fc} *(2 block plies at the center)* (from [5])	G_n^C	G_s^C
90 MPa	**50 KJ/m^2**	**130 KJ/m^2**	**0.2 KJ/m^2**	**1 KJ/m^2**

Table 2. Interface material properties (from [3])

G_n^C : Mode I fracture energy	G_s^C : Mode II fracture energy	N : tensile strength	S : Shear strength
0.2 KJ/m^2	**1 KJ/m^2**	**60 MPa**	**90 MPa**

Table 3. In-plane size effect

Laminate Lay-up	Experiment(MPa) and coefficient of variation (from [2])	Simulation (MPa) and % diff. with exp.
d=3.175mm, t=4mm, [45/90/-45/0]4s	478 (cv, 3.09%)	490 (+2.5%)
d=6.35mm, t=4mm, [45/90/-45/0]4s	433 (cv, 2.03%)	434 (+0.23%)
d=12.7mm, t=4mm, [45/90/-45/0]4s	374 (cv, 1.01%)	378 (+1.07%)

Table 4. Thickness size effect

Laminate Lay-up	Experiment(MPa) and coefficient of variation (from [2])	Simulation (MPa) and % diff. with exp.
d=3.175mm, t=1mm, [45/90/-45/0]s	570 (cv,7.69%)	573 (+0.5%)
d=3.175mm, t=2mm, [45/90/-45/0]2s	500 (cv, 3.95%)	493 (-1.4%)
d=3.175mm, t=4mm, [45/90/-45/0]4s	478(cv, 3.09%)	490 (+2.5%)

References

[1] S. R. Hallett, M. R. Wisnom. Experimental Investigation of Progressive Damage and the Effect of Layup in Notched Tensile Tests, *Journal of Composite Materials*, Vol. 40, pp 119-141, 2006.

[2] B.G. Green, M.R. Wisnom, S.R. Hallett. An experimental investigation into the tensile strength scaling of notched composites. *Composites: Part A*, Vol. 38, pp 867-878, 2007.

[3] S.R. Hallett, B.G. Green, W.G. Jiang, M.R. Wisnom. An experimental and numerical investigation into the damage mechanisms in notched composites. *Composites: Part A*, Vol. 40, pp 613-624, 2009.

[4] M.R. Wisnom, S.R. Hallett. Scalingeffects in notched composites. *Journal of Composite Materials*, Vol. 44, pp 195-210, 2010.

[5] M.J. Laffan, S.T. Pinho, P. Robinson, L.Iannucci. Measurement of the in situ ply fracture toughness associated with mode I fibre tensile failure in FRP. Part II: Size and lay-up effects. *Composite Science and Technology*, Vol. 70, pp 614-621, 2010.

[6] S.T. Pinho, P. Robinson, L. Iannucci. Fracture toughness of the tensile and compressive fibre failure modes in laminated composites. *Composite Science and Technology*, Vol. 66, pp 2069-2079, 2006.

[7] G. Catalanotti, P.P. Camanho, J. Xavier, C.G. Dávila, A.T. Marques. Measurement of resistance curves in the longitudinal failure of composites using digital image correlation. *Composite Science and Technology*, Vol. 70, pp 1986-1993, 2010.

[8] Stephen W. Tsai, Edward M. Wu. A general theory of strength for anisotropic materials. *Journal of Composite Materials*, Vol. 5, pp 58-80, 1971.

[9] Benzeggah ML, Kenane M. Measurement of mixed-mode delamination fracture toughness of unidirectional glass/epoxy composites with mixed-mode bending apparatus. *Composite Science and Technology*, Vol. 49, pp 439-449, 1996.

[10] M.R. Wisnom, B. Khan, S.R. Hallett. Size effects in unnotched tensile strength of unidirectional and quasi-isotropic carbon/epoxy composites. *Composite Structures*, Vol. 84, pp 21-28, 2008.

[11] M.R. Wisnom, S.R. Hallett. The role of delamination in strength, failure mechanism and hole size effect in open hole tensile tests on quasi-isotropic laminates. *Composites: Part A*, Vol. 40, pp 335-342, 2009.

[12] A. Turon, P.P. Camanho, J. Costa, J. Renart. Accurate simulation of delamination growth under mixed-mode loading using cohesive elements: Definition of interlaminar strengths and elastic stiffness. *Composite Structures*, Vol. 92, pp 1857-1864, 2010.

[13] A. Turon, C.G. Dávila, P. P. Camanho, J. Costa. An engineering solution for mesh size effects in the simulation of delamination using cohesive zone models. *Engineering Fracture Mechanics*, Vol. 74, pp 1665-1682, 2007.

[14] Giulio Alfano. On the influence of the shape of the interface law on the application of cohesive-zone models. *Composites Science and Technology*, Vol. 66, pp 723-730, 2006.

[15] P.P. Camanho, P. Maimí, C.G. Dávila. Prediction of size effects in notched laminates using continuum damage mechanics. *Composite Science and Technology*, Vol. 67, pp 2715-2727, 2007.

[16] Zdeněk P. Bažant, Qiang Yu. Universal size effect law and effect of crack depth on quasi-brittle structure strength, *Journal of Engineering Mechanics*, Vol. 135, pp 78-84, 2009.